Location of the Fisher-Widom line for systems interacting through short-ranged potentials

C. Vega,[1] L. F. Rull,[2] and S. Lago[1]
[1]*Departamento de Química Física, Facultad de Ciencias Químicas, Universidad Complutense, 28040, Madrid, Spain*
[2]*Departamento de Física Atómica Molecular y Nuclear, Universidad de Sevilla, Aptdo 1065, Sevilla 41080, Spain*
(Received 12 October 1994)

For finite-ranged potentials the behavior of the total correlation function $h(r)$ at large distances can be of two different types. In three-dimensional systems at low densities the function $r\,h(r)$ presents exponential decay whereas at high densities it presents exponentially damped oscillatory decay. The locus of points on the phase diagram where a transition from exponential to oscillatory decay occurs is denoted as the Fisher-Widom line after the work of these authors [M. E. Fisher and B. Widom, J. Chem. Phys. **50**, 3756 (1969)]. These authors exactly computed the Fisher-Widom line for several one-dimensional systems and conjectured that the same behavior could occur in three dimensions. In this work the Fisher-Widom line is computed for a three-dimensional finite-range potential by using the structural information obtained from the reference hypernetted chain theory which is probably the most successful theory of liquid structure available now. By combining these results with computer simulations of the vapor-liquid equilibria of the considered model the Fisher-Widom line is located within the phase diagram of the model. For the considered model the Fisher-Widom line cuts the liquid branch of the vapor liquid equilibria at a reduced temperature of $T/T_c=0.88$ and a reduced density of $\rho/\rho_c=2.07$. The effect of the range of the potential on the location of the Fisher-Widom line is also considered. Increasing the range of the potential reduces the region of the phase diagram where oscillatory behavior of the function $r\,h(r)$ occurs. The long-range decay of a Lennard Jones fluid is also considered. Decay of $h(r)$ to zero at large distances is different for a Lennard-Jones potential and for a finite-ranged potential. Although the Lennard Jones potential does not present a true Fisher-Widom line when the ultimate decay of $h(r)$ is considered it is shown that it exhibits a Fisher-Widom–like transition when an intermediate range of distances is considered.

PACS number(s): 61.20.−p

I. INTRODUCTION

The local density around a central particle can be described by introducing the pair correlation function [1] $g(r)$ which is just the ratio of the local number density at a distance r to the bulk number density ρ. Another useful function is the total correlation function $h(r)$ which is just $h(r)=g(r)-1$. For fluid phases (i.e., gas or liquid) and excluding the critical point, the function $h(r)$ tends to zero at large distances. An interesting problem is the asymptotic form of $h(r)$ at large values of r. When the particles of the system interact through a pair potential $u(r)$ which decays to zero more slowly than exponentially (i.e., the Lennard-Jones potential) then the asymptotic form of $h(r)$ is known [2–4].

When the potential is short ranged or decays to zero faster than an exponential, then a different behavior is obtained. In this case two different behaviors are obtained depending on the thermodynamic conditions (i.e., density and temperature). In a certain region of the phase diagram of the system the decay of $r^{(d-1)/2}h(r)$ to zero is exponential. In other regions, $r^{(d-1)/2}h(r)$ decays to zero in an exponentially damped oscillatory way. The dimensionality of the fluid is represented by d. The locus of points of the phase diagram where the transition from exponential to oscillatory decay occurs is denoted as the Fisher-Widom (FW) line after the work of these authors [5]. Fisher and Widom [5] were the first to propose and analyze this problem. They considered one-dimensional systems with nearest neighbor interactions (short-ranged potential) and showed that a locus of points of the phase diagram exists where the asymptotic behavior of $h(r)$ changes from exponential decay to damped oscillatory decay. For one-dimensional systems, decay of $h(r)$ at large r is determined by the pole λ_1 with the largest real part of the Laplace transform of $h(r)$. In case λ_1 is real then exponential decay occurs with decay length $-1/\lambda_1$ (λ_1 is negative). If λ_1 is complex then the complex conjugate λ_1^* is also a pole and oscillatory damped decay is found. Fisher and Widom determined the FW line for several one-dimensional systems [5]. By using the mean field approximation, these authors determined the vapor-liquid equilibria of the studied one-dimensional systems. These authors then combined the vapor-liquid equilibra results with the computed FW line, showing the regions of the phase diagram where exponential and oscillatory decay should occur. Fisher and Widom [5] conjectured that the FW line could also occur in three-dimensional systems, provided that the potential is short ranged, and that a similar plot to the one obtained by them for the one-dimensional system should be obtained. However, in their work [5] no result for a three-dimensional system was reported.

The problem of the determination of the FW line for three-dimensional systems interacting through a short-ranged potential has been recently considered [6,7]. In

fact, Evans and co-workers [6,7] have shown how to analyze the long-range behavior of $r\,h(r)$ for three-dimensional systems interacting through a short-ranged potential. Their approach to the problem is the use of the Ornstein-Zernlike equation [1]. The Ornstein-Zernlike equation is just a relation between $h(r)$ and the direct correlation function of the system $c(r)$. The analysis of Evans and co-workers [6,7] shows that the asymptotic form of $r\,h(r)$ at large r is dominated by the pole (purely imaginary or complex) of the structure factor $S(q=\alpha_1+i\alpha_0)$ with the smallest imaginary part. In case this pole is purely imaginary then exponential decay occurs with decay length $1/\alpha_0$, whereas if it is complex then exponentially damped oscillatory decay occurs with a wavelength of $2\pi/\alpha_1$ and a decay length of $1/\alpha_0$. The FW line is just the locus of points of the phase diagram where the purely imaginary pole ($\alpha_1=0$) of $S(q)$ and the complex pole of $S(q)$ with the smallest imaginary part have the same inverse decay length α_0. Evans and co-workers [6,7] showed that the knowledge of the direct correlation function $c(r)$ for every temperature and density of the phase diagram is enough for determining the FW line. For the square well system, the Fisher-Widom line has been computed [6,7] by using two different expressions for $c(r)$, namely the random phase approximation and $c(r)$ arising from the WDA density functional theory of Tarazona [8]. The vapor-liquid equilibria was also determined within the context of the density functional theory [6]. In this way the Fisher-Widom line was located within the phase diagram of the studied model. These works constitute the first reported determination of the FW line for a three-dimensional fluid. The picture emerging from those studies [6,7] is in agreement with that proposed by Fisher and Widom for one-dimensional systems [5]. Evans *et al.* [6] showed that the Fisher-Widom line intersects the liquid branch of the vapor-liquid equilibria at a reduced temperature of about $T/T_c=0.9$ where T_c is the critical temperature. Consequences of that on the density profile of vapor-liquid or wall-fluid interfaces were also analyzed [6,9].

During the last two decades great progress has been made on the statistical thermodynamics of spherical fluids [1,10]. One of the most successful theories is the reference hypernetted chain theory [11] (RHNC). In this theory, the Ornstein-Zernlike equation is solved along with the RHNC closure. The basic idea behind RHNC is the insensitivity of the bridge function [1] (the sum of the bridge diagrams) to the details of the potential. In this work we shall apply the RHNC integral equation to the determination of the Fisher-Widom line of a three-dimensional fluid. Since the RHNC is the most successful route to the thermodynamic and structural properties of spherical fluids, it is expected that $c(r)$ as determined from the RHNC theory will be quite accurate, and that will allow a very precise determination of the FW line. The effect of the range of the potential on the FW line will also be analyzed. In order to locate the FW line within the phase diagram of the model, vapor-liquid equilibria will be determined by computer simulation. We believe that this combination of RHNC results for determining the FW line and computer simulation to obtain the vapor-liquid envelope will provide a very precise determination of the location of the FW line within the phase diagram of the system. We expect qualitative agreement with previous results but higher accuracy in the location of the FW line.

The scheme of this work is as follows. In Sec. II the determination of the FW line as well as details of the numerical calculations are given. Section III presents the results, and in Sec. IV the conclusions of this work are given.

II. LOCATION OF THE FISHER-WIDOM LINE

We shall briefly outline the basic equations for the determination of the Fisher-Widom line of a three-dimensional system and we refer the reader to the original papers [5–7] for further details.

The Ornstein-Zernike (OZ) equation for a spherical fluid can be written as

$$h(r_{12})=c(r_{12})+\rho\int c(r_{13})h(r_{23})d\mathbf{r}_3 , \tag{1}$$

where ρ is the number density. The three-dimensional Fourier transform of a function $f(r)$ will be denoted as $\hat{f}(q)$ and is obtained from the relation

$$\begin{aligned}\hat{f}(q)&=\int \exp(i\mathbf{q}\cdot\mathbf{r})f(r)d\mathbf{r}\\&=4\pi\int rf(r)\sin(qr)/qdr .\end{aligned} \tag{2}$$

Then by taking the Fourier transform of the Ornstein-Zernike equation it can be rewritten as

$$\hat{h}(q)=\hat{c}(q)/[1-\rho\hat{c}(q)] . \tag{3}$$

By taking the inverse Fourier transform of $\hat{h}(q)$, then $h(r)$ can be obtained as

$$h(r)=[1/(2\pi^2)]\int_0^\infty q\hat{c}(q)/[1-\rho\hat{c}(q)]\sin(qr)/rdq . \tag{4}$$

Hence we obtain

$$r\,h(r)=[1/(2\pi^2)]\int_0^\infty q\hat{c}(q)/[1-\rho\hat{c}(q)]\sin(qr)dq . \tag{5}$$

Taking into account that $\hat{h}(q)$ is an even function of q then Eq. (5) can be rewritten as

$$r\,h(r)=[1/(4\pi^2 i)]\int_{-\infty}^{\infty} q\{\hat{c}(q)/[1-\rho\hat{c}(q)]\}\exp(iqr)dq . \tag{6}$$

From a physical point of view only real positive values of q have a physical meaning. From a mathematical point of view complex values of q are also allowed. Therefore, we shall consider complex values of q of the form

$$q=\alpha_1+i\alpha_0 . \tag{7}$$

By performing a contour integration in Eq. (6) on an infinite radius semicircle in the upper-half plane one obtains [7]

$$r\,h(r)=[1/(2\pi)]\sum_n \exp(iq_n r)R_n , \tag{8}$$

where q_n is the nth pole and R_n the residue of

$q\hat{c}(q)/[1-\rho\hat{c}(q)]$ at $q=q_n$. Poles of the function $q\hat{c}(q)/[1-\rho\hat{c}(q)]$) are obtained by solving the equation

$$1-\rho\hat{c}(q)=0 \ . \tag{9}$$

By equating imaginary and real parts in Eq. (9) the following equations are obtained:

$$\alpha_0=4\pi\rho\int rc(r)\sinh(\alpha_0 r)\cos(\alpha_1 r)dr \ , \tag{10a}$$

$$\alpha_1=4\pi\rho\int rc(r)\cosh(\alpha_0 r)\sin(\alpha_1 r)dr \ . \tag{10b}$$

Solving Eq. (9) is therefore equivalent to solving the pair of Eqs. (10). Two kinds of solutions to Eqs. (10) can be found [6,7]. The first kind of solution has $\alpha_1=0,\alpha_0\neq 0$ and yields an exponential decay contribution to $r\,h(r)$ [see Eq. (8)]. A second kind of solution is obtained with $\alpha_1\neq 0$ and $\alpha_0\neq 0$. In that case poles occur in conjugate pairs $q=\pm\alpha_1+i\alpha_0$. The contribution of a conjugate pair to $r\,h(r)$ is that of an exponentially damped (with inverse decay length α_0) oscillatory (sinusoidal) function. Therefore the behavior of $r\,h(r)$ at large values of r is dominated by the solution of Eqs. (10) with the smallest value of α_0. The FW line is just the locus of points on the phase diagram where the purely imaginary solution and the complex solution with the smallest imaginary part have the same value of α_0. It is clear from Eqs. (10) that determination of the FW line requires only the knowledge of $c(r)$ at every temperature and density.

In order to obtain the FW line we shall solve the OZ equation [Eq. (1)] along with the RHNC closure. The RHNC closure [11] is given by

$$c(r)=h(r)-\ln\{[h(r)+1]\exp[u(r)/(kT)]\}+B_0(r) \ , \tag{11}$$

where B_0 is the bridge function [1] of the reference system. In this work we shall take the hard sphere (HS) as the reference system so that

$$B_0(r,\rho,T)=B_{\rm HS}(r,\rho;d_{\rm HS}) \ . \tag{12}$$

The diameter of the equivalent hard sphere is obtained by solving the condition [11]

$$\rho\int[g(r,\rho T)-g_{\rm HS}(r,\rho;d_{\rm HS})][dB_{\rm HS}(r)/d(d_{\rm HS})]dr=0 \ . \tag{13}$$

If the diameter of the hard sphere $d_{\rm HS}$ is obtained from the solution of Eq. (13) then pressures obtained from the virial theorem and from derivation of the free energy are identical [11]. Therefore the use of Eq. (13) to obtain $d_{\rm HS}$ provides thermodynamic consistency between these two routes. In order to solve Eq. (13) the bridge function of hard spheres is needed. We shall use the parametric form proposed by Labik and Malijevsky [12,13]. This parametrization has proved to be quite accurate in a number of works involving different kinds of potentials [14–17]. Equation (1) along with Eqs. (11)–(13) constitute the RHNC theory. The RHNC integral equation is solved by using the algorithm proposed by Labik, Malijevsky, and Vonka [18]. We typically used a grid with $N=4096$ points, $M=250$ points, and $\Delta r=0.01\sigma$. By solving the RHNC integral equation the direct correlation function $c(r)$ is obtained at every density and temperature. Once $c(r)$ is known from the RHNC theory then we looked for solutions of Eqs. (10). We typically solve the RHNC equation for about 20 densities at every temperature. In this way the density of the FW line for the considered temperature was obtained. Ten different temperatures were considered.

In this work we shall consider a short-ranged potential hereinafter denoted as SLJ. The pair potential $u_{\rm SLJ}$ for the SLJ model is given by

$$u_{\rm SLJ}(r)=4\varepsilon[(\sigma/r)^{12}-(\sigma/r)^6]\theta(r-r_c) \ , \tag{14}$$

$$\theta(x)=\begin{cases}1/\{1+\exp[-x/(x^2-\Delta^2)]\}, & |x|<\Delta \qquad (15)\\ 1, \quad x\leq-\Delta, \quad \theta(x)=0, \quad x\geq\Delta \ . & (16)\end{cases}$$

The value of Δ was set to 0.5σ. Most of the calculations were performed with $r_c=2.5\sigma$. However some calculations for $r_c=5\sigma$, $r_c=7.5\sigma$, $r_c=10\sigma$, and $r_c=20\sigma$ were also performed. The potential given by Eqs. (14)–(16) vanish at $r_c+\Delta$ as well as all its derivatives. The range of the potential is $r_c+\Delta$. The potential described by Eqs. (14)–(16) can be considered as a modified Lennard-Jones (LJ) potential with finite range and continuous derivatives at any value of r.

One of the aims of this work is to locate the position of the FW line within the phase diagram of the considered model. We would like to plot the FW line reduced by the critical magnitudes of the model. Although solution of the RHNC is always found at the densities where the FW line occurs, there is a region of the phase diagram where no solution of the RHNC is found (see the next section). The problem of the existence of a region where no solution of the OZ integral equation is found has been recently discussed in a number of papers [16,19–23]. For the LJ potential Lomba found that the region of no solution of the RHNC integral equation includes the critical point [16]. That precludes the determination of the critical point of the fluid within the RHNC theory. Similar conclusions were obtained in this work for the SLJ potential. Therefore determination of the critical point within the RHNC theory is not possible. To overcome this problem we have performed Gibbs ensemble simulations [24,25] of the considered $u_{\rm SLJ}$ potential. We refer the reader to the original papers of Panagiotopoulos and co-workers [24,25] for an explanation of the Gibbs ensemble simulation methodology. Details of the simulations are similar to those used in our previous work [26,27]. A total number of 512 particles were used. After 5000 cycles for equilibrium, 10 000 additional cycles were performed to compute thermodynamic averages. In this way the vapor-liquid equilibria of the SLJ model have been calculated. The critical point can be estimated from the coexistence envelope by using the rectilinear diameters law [28] (including a second order term in temperature) and the critical exponent $\beta=\frac{1}{3}$. In this way a reliable estimation of the critical point was obtained.

In order to assess the quality of the structural data provided by the RHNC theory we have performed some additional NVT Monte Carlo (MC) simulations of the SLJ

potential for the isotherm $T^*=T/(\varepsilon/k)=1.40$ and the densities $\rho^*=\rho\sigma^3=0.20$, 0.65. These runs will also be useful to validate the predictions of the RHNC theory concerning the determination of the FW line. In these MC runs we used 864 particles for $\rho^*=0.20$ and 1372 for $\rho^*=0.65$. This rather large number of particles was used in order to analyze the behavior of $h(r)$ at large values of r. In the next section results for the different considered models are presented.

III. RESULTS

We shall start presenting the results for the SLJ model with $r_c=2.5\sigma$. In Fig. 1 the values of α_0 for the imaginary pole and for the complex pole with the smallest value of α_0 are presented as a function of the density for the reduced temperature $T^*=1.4$. For the reduced density $\rho^*_{FW}=0.562$ the value α_0 of both poles is the same and, therefore, this state is on the FW line. For densities larger than ρ^*_{FW} exponentially damped oscillatory decay occurs. For densities less than ρ^*_{FW} the imaginary pole has the smallest value of α_0 and therefore $r\,h(r)$ presents exponential decay. In Fig. 2 the function $r^*\,h(r)$ is plotted for a density below the FW line and for a density above the FW line. The reduced distance r^* is defined as $r^*=r/\sigma$. In the first case exponential decay is clearly visible, whereas in the second case oscillatory damped decay is observed. Therefore, our determination of the FW line is consistent with the structural data presented in Fig. 2. In Fig. 3 the function $\ln[r^*h(r)]$ is plotted as a function of r^* for $\rho^*=0.20$ and $T^*=1.40$, which is a state below the FW line. Linear behavior is obtained at large values of r and that indicates exponential decay of $r^*h(r)$ at large r. A least squares fit to the values of $\ln[r^*h(r)]$ at large values yields a slope of -0.7812. This is in excellent agreement with the value α_0 of the imaginary pole computed from the solution of Eqs. (10) which is $\alpha_0=0.7809$. This further shows how the behavior of $r^*h(r)$ at large distances is given by the solution of Eqs. (10).

To assess the quality of the structural data provided by RHNC we compare in Fig. 4 the radial distribution $g(r)$ obtained from the solution of the integral equation with $g(r)$ obtained from NVT MC simulations. Two densities were chosen for this comparison. One below the FW line and another above the FW line. The agreement between

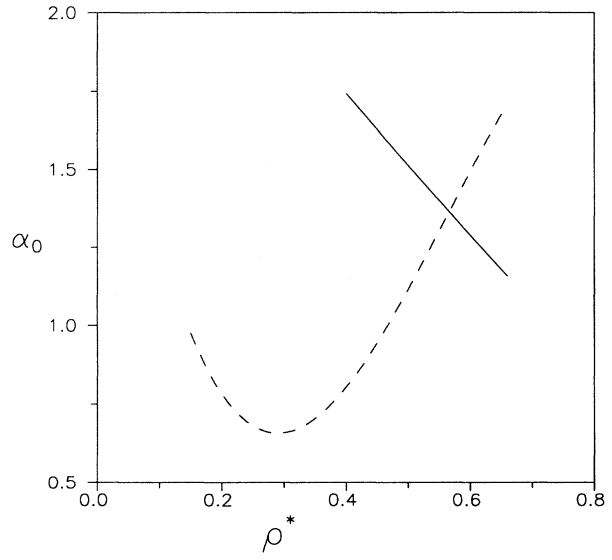

FIG. 1. Imaginary part α_0 for the purely imaginary pole (dashed line) and for the complex pole with the smallest value of α_0 (solid line) as a function of the reduced density ρ^* for the SLJ model with $r_c=2.5\sigma$ and $\Delta=0.5\sigma$. Results correspond to the isotherm $T^*=1.40$.

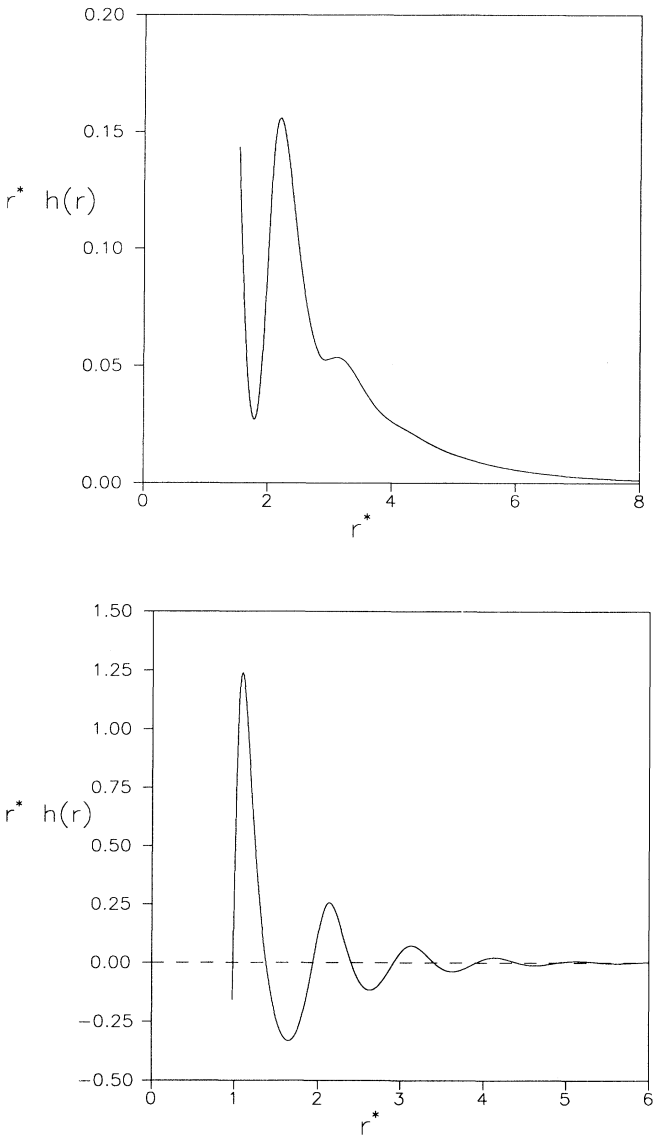

FIG. 2. Behavior of $r^*h(r)$ as a function of r^* for a density below the FW line and for a density above the FW line. The reduced r^* is defined as $r^*=r/\sigma$. The $h(r)$ function was obtained from the solution of the RHNC integral equation for the SLJ model with $r_c=2.5\sigma$ and $\Delta=0.5\sigma$. The considered temperature in both cases is $T^*=1.4$. (a) Density below the FW line, $\rho^*=0.20$. (b) Density above the FW line $\rho^*=0.65$.

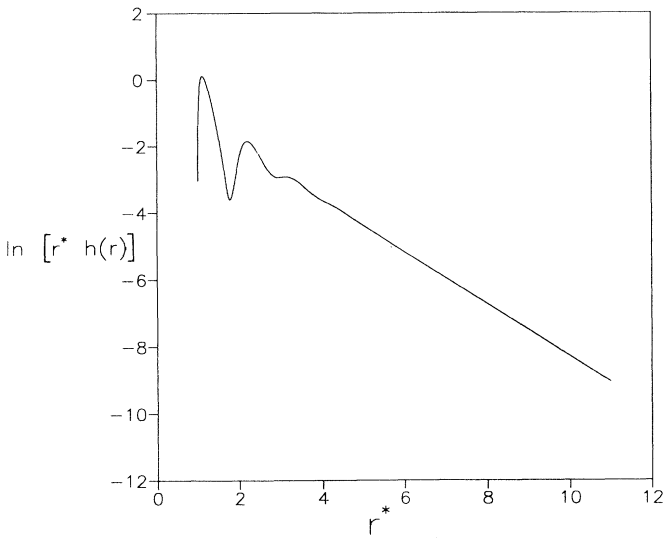

FIG. 3. The function $\ln[r^* h(r)]$ from RHNC versus r for the SLJ model with $r_c=2.5\sigma$ and $\Delta=0.5\sigma$. Results correspond to $\rho^*=0.20$ and $T^*=1.4$.

theoretical and simulation results presented in Fig. 4 is excellent. That gives us some confidence in our estimation of the FW line for the considered model. Moreover, the MC data are consistent with the theoretical predictions. MC results presented in Fig. 4(a) present exponential decay and in Fig. 4(b) present exponentially damped oscillatory decay. The FW line must be between these two densities which is consistent with our calculated value ρ^*_{FW}. It should be mentioned that since we used NVT simulations, the asymptotic value of $g(r)$ from simulations is not one but $1-1/N_p$ where N_p is the number of particles used in the simulations (864 at the smallest density and 1372 at the highest density).

In Table I densities of the FW line at several temperatures are given for the SLJ model with $r_c=2.5\sigma$. Note that for the SLJ model with $r_c=2.5\sigma$ densities along the FW line decrease as the temperature increases.

In Table II vapor-liquid equilibria for the SLJ system with $r_c=2.5\sigma$ obtained from Gibbs ensemble simulations are shown. Note that pressure computed via the virial theorem in the gas and liquid phases is almost the same which constitutes a cross checking of the calculations. The estimated critical point obtained from the Gibbs ensemble results is $T^*_c=1.178$ and $\rho^*_c=0.298$. In Fig. 5(a) the coexistence densities for that model are presented along with the computed value of the FW line. The FW line intersects the liquid branch of the coexistence curve. The critical point belongs to the region of purely exponential decay. Results presented in Fig. 5(a) are consistent with the previous work of Fisher and Widom [5] and of Evans *et al.* [6]. In Fig. 5(b) a corresponding states plot of the vapor-liquid equilibria and of the FW line is presented. The FW line cuts the liquid branch of the vapor-liquid equilibria at the reduced temperature of $T/T_c=0.88$ and the reduced density of $\rho/\rho_c=2.07$. Our corresponding states plot presented in Fig. 5(b) is in agreement with the previous results of Evans *et al.* [6] for the square well potential obtained by using a less accurate approximation of $c(r)$. Results presented so far give further support to the existence of the FW line for short-ranged three-dimensional potentials having both repulsive and attractive forces. Our results confirm previous predictions [5,6] of the fact that the FW lines cuts the liquid branch of the vapor-liquid equilibria at a temperature relatively close to the critical temperature. Note that according to the results presented in Fig. 5(b) that for temperatures less than $T/T_c=0.88$, gas and liquid at coexistence present different behaviors of the function $r\,h(r)$ at large distances. Exponential decay is found for the gas whereas exponentially damped oscillatory decay is found for the liquid. According to Evans *et al.* [6], an

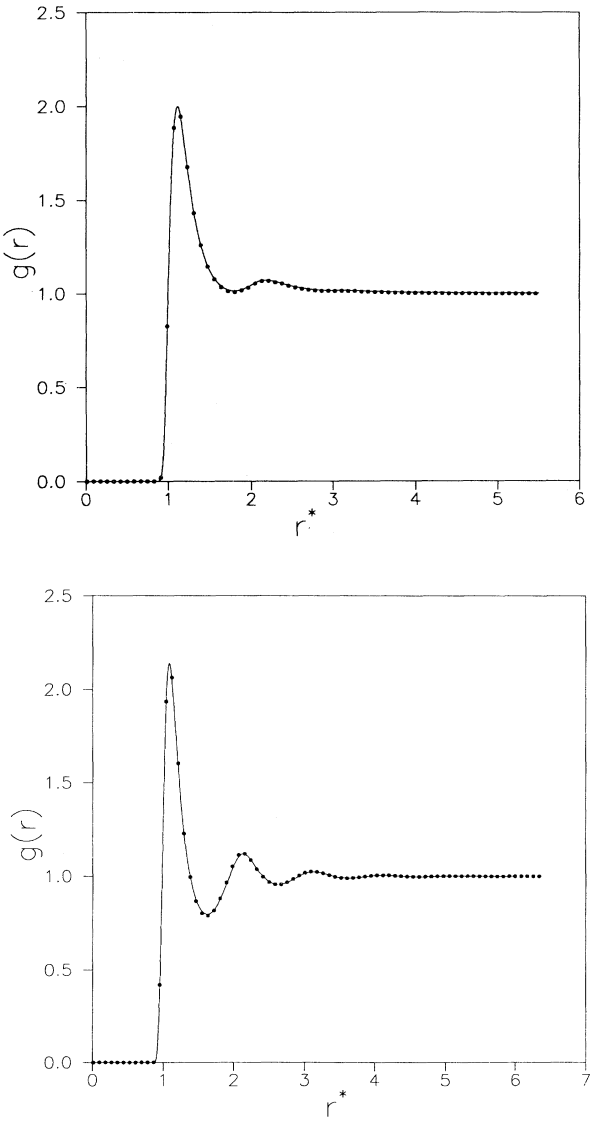

FIG. 4. Simulation and theoretical results for $g(r)$ at two different densities below and above the FW line. Results correspond to the SLJ model with $r_c=2.5\sigma$ and $\Delta=0.5\sigma$ at $T^*=1.40$. Solid line, RHNC results; points, MC results. (a) Reduced density $\rho^*=0.20$. (b) Reduced density $\rho^*=0.65$.

TABLE I. Fisher-Widom line for the SLJ model with several values of r_c as obtained from the solution of Eqs. (10). Direct correlation function $c(r)$ was taken from the RHNC theory. The value of Δ was of $\Delta=0.5\sigma$.

T^*	$r_c=2.5\sigma$	$r_c=5\sigma$	$r_c=7.5$	$r_c=10\sigma$	$r_c=20\sigma$
5.0	0.39	0.60	0.74	0.83	
2.0	0.50	0.61	0.67	0.74	0.90
1.90	0.51	0.61	0.68	0.74	0.88
1.80	0.52	0.62	0.68	0.74	0.87
1.70	0.53	0.63	0.68	0.73	0.87
1.60	0.54	0.63	0.67	0.73	0.85
1.50	0.55	0.63	0.68	0.73	0.85
1.40	0.56	0.64	0.68	0.73	0.84
1.30	0.58	0.65	0.68	0.72	
1.20	0.59	0.653	0.686	0.73	0.83
1.10	0.61	0.666	0.693	0.72	
1.00	0.62	0.675	0.694	0.72	0.813
0.90		0.688		0.73	
0.80		0.7031			

important consequence of that is that for T/T_c less than 0.88 the density profile of a vapor-liquid interface should have oscillations on the liquid branch.

In Fig. 5 the region where no solution of the RHNC equation is found is presented. Note that this region includes the critical point of the model. The same problem was previously found by Lomba [16] for the full LJ potential and seems to be a general failure of the RHNC theory. However, the FW line is located in the region where solution of the RHNC equation exists so that it can be readily computed by using the structural output of the integral equation.

Finally, the effect of the range of the potential on the FW line will be analyzed. For that purpose the FW line has been computed for the SLJ model with $r_c=5\sigma$, $r_c=10\sigma$, and $r_c=20\sigma$. Results are given in Table I. It is observed that as the value of r_c increases the FW line moves to higher densities. For $r_c=20\sigma$, $T^*=5$, and $\rho^*=0.90$ exponential decay is found. We fail to find a solution of the RHNC equation for this model and temperature at higher densities. We have not computed the vapor-liquid equilibria of the SLJ models with $r_c=5\sigma$, $r_c=10\sigma$, or $r_c=20\sigma$. However, it is expected that for these rather large values of the range of the potential, namely 5.5σ, 10.5σ, and 20.5σ, respectively, the vapor-liquid equilibria of the SLJ models will be very close to that of a Lennard-Jones system. The vapor-liquid equilibria of the Lennard-Jones potential is well known from

TABLE II. Gibbs ensemble results for the SLJ with $r_c=2.5\sigma$ and $\Delta=0.5\sigma$. Digits in parentheses show the uncertainty of the last reported digits. Pressures are given in units of ε/σ^3. Reduces densities ρ^* are defined as $\rho^*=\rho\sigma^3$. Reduced temperature is given by $T^*=T/(\varepsilon/k)$. The subindices g and l refer to gas and liquid phase results, respectively.

T^*	ρ_g^*	p_g	ρ_l^*	p_l
0.85	0.018(2)	0.0137(9)	0.741(9)	0.011(5)
0.90	0.026(1)	0.020(1)	0.710(19)	0.018(130)
1.00	0.056(5)	0.041(3)	0.650(16)	0.035(55)
1.03	0.066(5)	0.049(3)	0.627(17)	0.045(50)
1.05	0.071(6)	0.052(4)	0.604(23)	0.052(49)
1.08	0.098(11)	0.066(5)	0.582(23)	0.063(50)
1.10	0.105(8)	0.071(5)	0.560(26)	0.067(38)
1.14	0.141(21)	0.087(8)	0.490(45)	0.088(36)
1.15	0.154(21)	0.092(8)	0.451(80)	0.094(35)

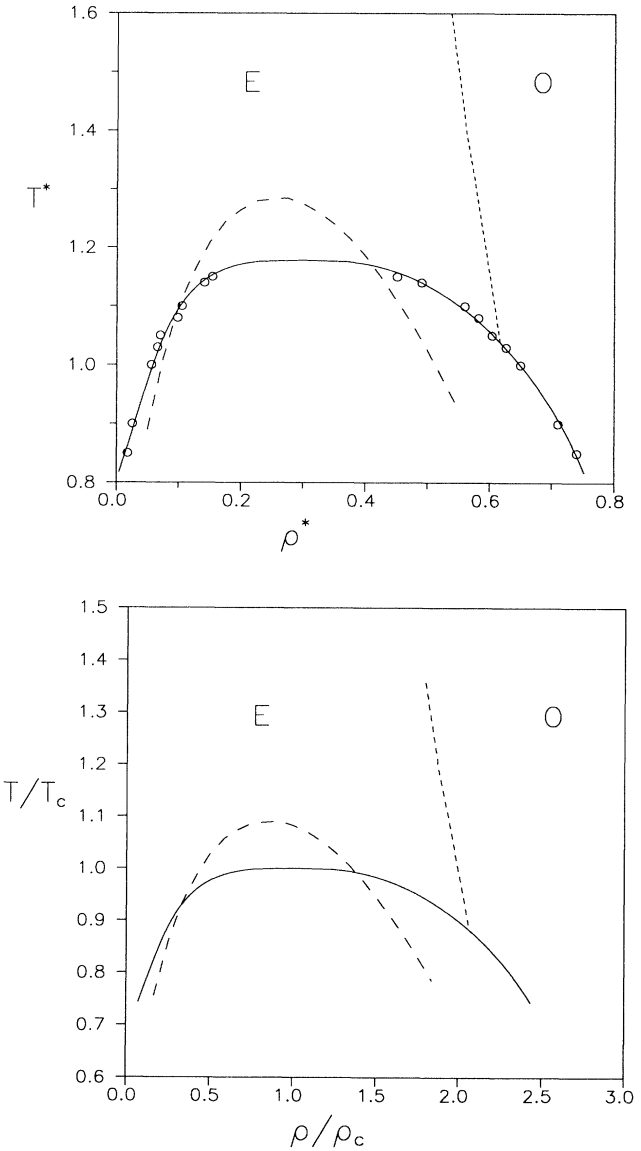

FIG. 5. FW line and vapor-liquid equilibria of the SLJ model with $r_c=2.5\sigma$ and $\Delta=0.5\sigma$. The FW line (short dashed line) was obtained from the structural results of the RHNC equation. Coexistence densities (open circles) were obtained from Gibbs ensemble simulation. The solid line is a fit to the Gibbs ensemble results. In the region labeled as E exponential decay of $r\,h(r)$ occurs whereas in the region labeled as 0 damped oscillatory decay occurs. The dashed line indicates the region of the phase diagram where no solution of the RHNC is found. (a) Reduced temperature versus reduced density. (b) Corresponding states plot of the results presented in (a).

computer simulations [29]. The same is true for the fluid-solid equilibria of this model [30]. In Fig. 6(a) the FW lines for $r_c=5\sigma$, $r_c=10\sigma$, and $r_c=20\sigma$ are plotted along with the vapor-liquid equilibria of the full LJ system. In Fig. 6(b) the same results are presented but are reduced by the critical properties of the LJ system. The slope of the FW line is negative for r_c less than 7.5σ and positive for larger values. Figure 6 shows that the region of the phase diagram where exponential decay occurs increases considerably with the range of the potential. In order to understand this behavior we shall briefly consider the case of a full LJ potential without any truncation.

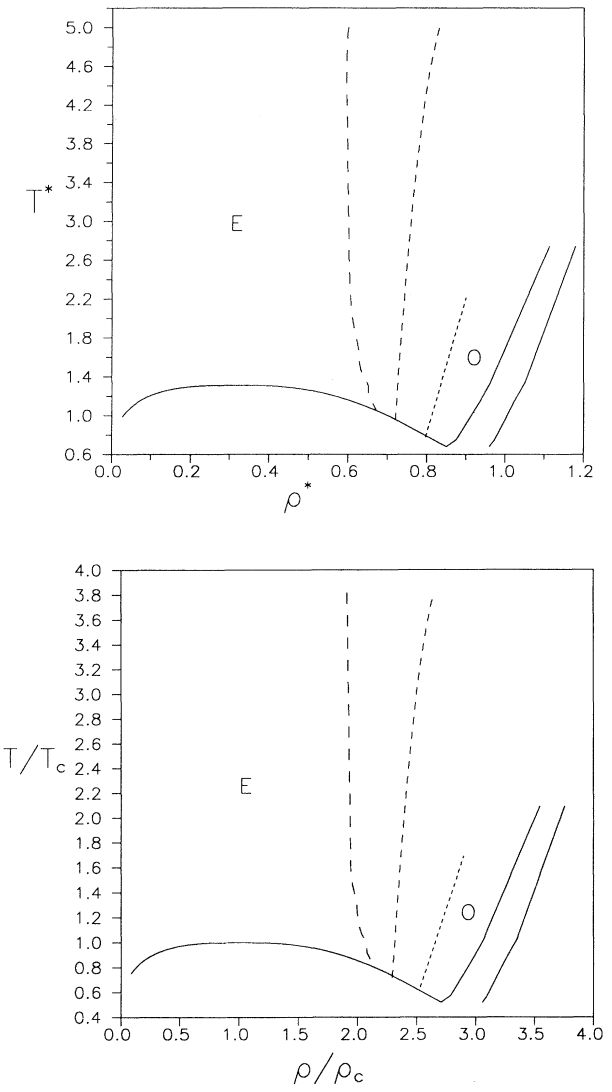

FIG. 6. FW line and vapor-liquid equilibria of the SLJ model with $r_c=5\sigma$ (long dashed), $r_C=10\sigma$ (dashed), and $r_c=20\sigma$ (short dashed line) determined from the RHNC theory. In all cases, the value $\Delta=0.5\sigma$ was used. Vapor-liquid coexistence densities (solid line) were taken from computer simulations of Ref. [29] for the full LJ potential. Liquid-solid coexistence densities from Monte Carlo results of Ref. [30] for the full LJ system are also included (solid lines on the right-hand side). Regions with exponential and oscillatory damped decay are labeled as *E* and *O*, respectively. (a) Reduced temperature versus reduced density. (b) Corresponding states plot of the results presented in (a).

The LJ potential can be obtained from Eq. (14) by removing the function $\theta(r-r_c)$. It is generally accepted that for a LJ potential the behavior of $c(r)$ at large distances is given by [4,10]

$$c(r)\approx 4\varepsilon(\sigma)^6/(kT\,r^6)\ . \tag{17}$$

A consequence of Eq. (17) is that the asymptotic behavior of $h(r)$ must be given by [3]

$$r^*h(r)\approx 4[S(0)]^2/(T^*r^{*5})\ , \tag{18}$$

where $S(0)$ is the structure factor at $q=0$

$$S(0)=1+4\pi\rho\int_0^\infty h(r)r^2dr\ . \tag{19}$$

By taking logarithms on both sides of Eq. (18) it can be rewritten as

$$\ln[r^*h(r)]=\{2\ln[S(0)]+\ln(4/T^*)\}-5\ln(r^*)\ . \tag{20}$$

We have solved the RHNC equation for the full LJ potential. For the LJ model we used a grid of $N=16384$ points, $M=1500$ points, and $\Delta r=0.025\sigma$. Our purpose is to check if the solutions of the RHNC equation satisfy Eqs. (17)–(18). For a few selected states we plot $\ln(c)$ versus $\ln(r^*)$ for large values of r and found linear behavior with a slope very close to -6. At large distances, the function $h(r)$ obtained from the RHNC equation was fitted to the expression

$$\ln[r^*h(r)]=c_1+c_2\ln(r^*)\ . \tag{21}$$

In Table III the coefficients of the fit c_1 and c_2 for the LJ model at several thermodynamic states obtained from the RHNC equation are presented. The slope of the fit, c_2 is

TABLE III. Structural results of the solution of the RHNC for the LJ potential. At large values of r we fitted our results of $r^*h(r)$ to the expression of Eq. (21) where $r^*=r/\sigma$. Values of c_1 and c_2 are shown. We also computed the expression $2\ln[S(0)]+\ln(4/T^*)$ which according to Eq. (20) should be equal to c_1. $S(0)$ is the calculated structure factor.

ρ^*	T^*	$S(0)$	$2\ln[S(0)]$ $+\ln(4/T^*)$	c_1	c_2
0.10	1.5	1.739	2.088	2.116	−5.00
0.15	1.5	2.358	2.697	2.751	−5.00
0.20	1.5	3.126	3.260	3.335	−5.01
0.25	1.5	3.636	3.562	3.726	−5.02
0.30	1.5	3.313	3.377	3.936	−5.10
0.35	1.5	2.536	2.842	3.643	−5.16
0.40	1.5	1.572	1.886	2.137	−5.03
0.45	1.5	0.916	0.804	0.958	−5.02
0.50	1.5	0.588	−0.082	0.053	−5.02
0.55	1.5	0.344	−1.153	−1.084	−5.01
0.60	1.5	0.234	−1.924	−1.633	−5.07
0.40	3.0	0.453	−1.295	−1.275	−5.00
0.40	2.5	0.519	−0.840	−0.783	−5.00
0.40	2.0	0.687	−0.057	−0.043	−5.01
0.40	1.5	1.572	1.886	2.137	−5.03

in all the cases very close to -5 as suggested by Eq. (20). The coefficient c_1 is in general close to the term in brackets of Eq. (20) except for the density $\rho^*=0.30$ which is very close to the critical density of the LJ system. Results presented in Table III show that the long-range decay of $h(r)$ for a LJ fluid is of the form of Eq. (18).

We have so far discussed results for the finite-range potential u_{SLJ} with several values of r_c and for the full LJ potential. It is obvious that there should be a connection between the structure of these two models since the u_{SLJ} tends to a LJ potential when r_c of the SLJ model goes to infinity. How is such a link made? To answer this question we considered the u_{SLJ} model with a relatively large value of r_c. We chose $r_c=20\sigma$. We shall analyze the results of this model obtained from the solution of the RHNC equation. Two different densities, $\rho^*=0.10$ and $\rho^*=0.60$, are considered within the isotherm $T^*=2$. In Fig. 7(a) $\ln[r^*h(r)]$ is plotted versus r^* for the two considered densities. In Fig. 7(b) $\ln[r^*h(r)]$ is plotted versus $\ln(r^*)$. Let us first consider the results for the smallest density [dashed lines in Figs. 7(a) and 7(b)]. For this density two different regimes in the behavior of $h(r)$ are clearly visible. From $r^*=13$ up to $r^*=20$ the decay of $h(r)$ approximately follows a power law given by Eq. (18) and that explains the linear region found in Fig. 7(b). For larger values of r decay of $r\,h(r)$ is exponential and that explains the linear region found in Fig. 7(a) for $r^*>27$. For the largest density (solid line in Fig. 7) the same behavior is found, although the linear region in Fig. 7(b) is found only between $r^*=12$ and $r^*=15$ and in Fig. 7(a) for $r^*>30$. For both densities the ultimate decay of $r\,h(r)$ follows an exponential law. Figure 7 describes how the transition from a SLJ to a LJ model occurs. For a SLJ model with a large value of r_c the following sequence in the structure is expected. For large values of r but less than r_c the behavior of $r\,h(r)$ should be approximately given by Eq. (18). For values of r much larger than r_c, exponential decay or exponentially damped oscillatory decay will occur depending on the location of the FW line for the considered SLJ model. In Fig. 6 it was shown that the FW line of the SLJ potential moves to higher densities as r_c increases and its slope becomes positive. Note that the slope of the fluid-solid coexistence curve presented in Fig. 6 is also positive. It seems reasonable to assume that for a sufficiently large value of r_c the FW line will be located within the fluid-solid coexistence region. In that case the whole phase diagram of the SLJ model will fall within the exponential decay region. In other words, for sufficiently large values of r_c decay of $r\,h(r)$ will follow a power law for r less than r_c and exponential decay for larger values. Therefore there should be a crossover from power law decay to exponential decay at large distances. Note that both the power law and the exponential decay go to zero through positive values. It may look surprising that for the SLJ system with a large value of r_c a range of distances exist where the decay of $r\,h(r)$ follows a power law. It has recently been shown [31] that the number of complex poles of a finite-ranged potential significantly increases with the range of the potential. All these poles present similar values of α_0 and therefore of the exponential decay length α_0^{-1}. Hence, although Eq. (8) is valid it is necessary to include a large number of terms in order to describe the behavior of $h(r)$ at distances less than the range of the potential. The power law decay appearing for distances less than r_c arises from the combination of a large number of exponentially damped sinusoidal functions. From a mathematical point of view it is possible to fit the function r^{-5} in a finite interval as a combination of a large number of exponentially damped sinusoidal functions.

When considering the ultimate decay of $h(r)$ we conclude that the SLJ potential with very large r_c presents exponential decay through the whole fluid phase. The full LJ presents power law decay through the whole fluid phase. None of these models present a true FW line. In

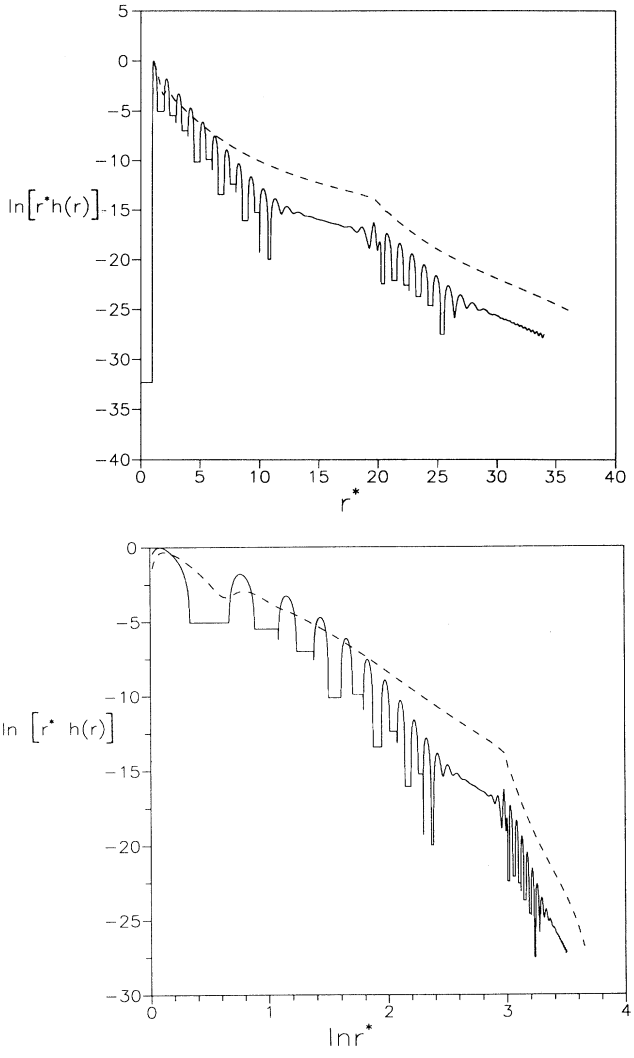

FIG. 7. Structure of the SLJ with $r_c=20\sigma$ as obtained from the RHNC equation. The considered temperature is $T^*=2$. Dashed line, $\rho^*=0.10$, solid line, $\rho^*=0.60$. For the largest density the horizontal lines represent regions where $h(r)$ takes negative values. (a) Plot of $\ln[r^*h(r)]$ versus r^*. (b) Plot of $\ln[r^*h(r)]$ versus $\ln(r^*)$.

the SLJ model this is due to the fact that the FW line falls at densities beyond the freezing transition. However when considering the intermediate behavior of $h(r)$ then the SLJ model and the full LJ model behave quite similarly. Evans *et al.* [7] have pointed out that for an infinite-range potential as the LJ system there can be a FW-like line when the behavior of $r\,h(r)$ at intermediate range is considered. This was illustrated by Sung and Chandler [32] by presenting the results of $h(r)$ at the intermediate range obtained from application of the optimized cluster theory. Our results also support the appearance of a FW-like line for the SLJ system with very large r_c when the intermediate range of the potential is considered. In fact, in Fig. 7(a) it is shown that although the ultimate decay of $r\,h(r)$ is exponential in both cases, when considering the intermediate range, it could be said that the lower density $\rho^*=0.10$ has intermediate exponential decay whereas the highest density $\rho^*=0.60$ presents exponentially damped oscillatory decay. In a recent paper, Carvalho *et al.* [31] have analyzed this point in detail. In this paper, however, we focused in the behavior of the ultimate decay of $h(r)$ and therefore it must be concluded that in that respect the SLJ model and the LJ model behave in a different way.

IV. SUMMARY AND CONCLUSIONS

The FW line has been determined for a finite-range potential (SLJ) by using the direct correlation function $c(r)$ as obtained from the RHNC integral equation. In addition, the vapor-liquid equilibria for the same potential have been computed by using Gibbs ensemble simulations. For the SLJ model with $r_c=2.5\sigma$, the FW line cuts the vapor-liquid equilibria when $T/T_c=0.88$. Structural information obtained from computer simulation is consistent with the existence of a transition in the behavior of the function $r\,h(r)$ at large distances. At low densities exponential decay of the function $r\,h(r)$ is found, whereas at large densities exponentially damped oscillatory decay occurs. All our results give further support to the presence of a FW line in three dimensions for finite-range potentials, provided that the pair potential has repulsive and attractive forces. In addition to that, results of this work probably provide the most accurate determination of the FW line so far presented for a three dimensional system. This previous statement is supported by the excellent agreement found between computer simulation and RHNC theory for the function $h(r)$ at several densities.

When the range of the potential increases while remaining finite, the region of the phase diagram presenting exponential decay significantly increases. Our results strongly suggest that for potentials with a finite but very long range, the FW line occurs at densities beyond the freezing transition. Therefore, in that case the whole fluid presents exponential decay at very large distances. For these systems the following sequence in the decay of $r\,h(r)$ is observed. For large distances but less than the range of the potential, the decay of $r\,h(r)$ follows a power law. For distances much larger than the range of the potential, exponential decay occurs.

Neither the LJ potential nor the SLJ potential with very large r_c have a FW line within the fluid phase region. The explanation of that is different in each case. However, when the intermediate range of distances is considered, then, the LJ model and the SLJ model with large r_c present a FW-like line.

ACKNOWLEDGMENTS

This work was financially supported by project Nos. PB91-0364 and PB91-602 of the Spanish DGICYT (Direccion General de Investigación Científica y Técnica). We thank M. E. Fisher for suggesting the study of the potential considered in this work and for very helpful correspondence. We thank R. J. F. Leote de Carvalho and R. Evans for sending their manuscript (Ref. [31]) prior to publication and for helpful correspondence.

[1] J. P. Hansen and I. R. McDonald, *Theory of Simple Liquids*, 2nd ed. (Academic, London, 1986).
[2] B. Widom, J. Chem. Phys. **41**, 74 (1964).
[3] J. E. Enderby, T. Gaskell, and N. H. March, Proc. Phys. Soc. **85**, 217 (1965).
[4] M. D. Johnson, P. Hutchinson, and N. H. March, Proc. R. Soc. A **282**, London Ser. 283 (1964).
[5] M. E. Fisher and B. Widom, J. Chem. Phys. **50**, 3756 (1969).
[6] R. Evans, J. R. Henderson, D. C. Hoyle, A. O. Parry, and Z. A. Sabeur, Mol. Phys. **80**, 755 (1993).
[7] R. Evans, R. J. F. Leote de Carvalho, J. R. Henderson, and D. C. Hoyle, J. Chem. Phys. **100**, 591 (1994).
[8] P. Tarazona, Phys. Rev. A **31**, 2672 (1985).
[9] R. Evans, D. C. Hoyle, and A. O. Parray, Phys. Rev. A **45**, 3823 (1992); see also, J. R. Henderson and Z. A. Sabeur, J. Chem. Phys. **97**, 6750 (1992).
[10] C. G. Gray and K. E. Gubbins, *Theory of Molecular Fluids* (Clarendon, Oxford, 1984).
[11] F. Lado, S. M. Foiles, and N. W. Ashcroft, Phys. Rev. A **45**, 2374 (1983).
[12] A. Malijevsky and S. Labik, Mol. Phys. **60**, 663 (1987).
[13] S. Labik and A. Malijevsky, Mol. Phys. **67**, 431 (1989).
[14] C. Vega and S. Lago, Mol. Phys. **72**, 215 (1991).
[15] C. Vega and S. Lago, J. Chem. Phys. **94**, 310 (1991).
[16] E. Lomba, Mol. Phys. **68**, 87 (1989).
[17] E. Lomba and N. G. Almarza, J. Chem. Phys. **100**, 8367 (1994).
[18] S. Labik, A. Malijevsky, and P. Vonka, Mol. Phys. **56**, 709 (1985).
[19] L. Belloni, J. Chem. Phys. **98**, 8080 (1993).
[20] P. G. Ferreira, R. L. Carvalho, M. M. Telo de Gama, and A. G. Schlijper, J. Chem. Phys. **101**, 594 (1994).
[21] A. G. Schlijper, M. M. Telo da Gama, and P. G. Ferreira, J. Chem. Phys. **98**, 1534 (1993).
[22] J. J. Brey and A. Santos, Mol. Phys. **57**, 149 (1986).

[23] J. A. Anta, E. Lomba, and M. Lombardero, Phys. Rev. E **49**, 402 (1994).
[24] A. Z. Panagiotopoulos, Mol. Phys. **61**, 813 (1987).
[25] A. Z. Panagiotopoulos, N. Quirke, M. Stapleton, and D. J. Tildesley, Mol. Phys. **63**, 527 (1988).
[26] C. Vega, S. Lago, E. de Miguel, and L. F. Rull, J. Phys. Chem. **96**, 7431 (1992).
[27] E. de Miguel, L. F. Rull, M. Chalam, and K. E. Gubbins, Mol. Phys. **71**, 1223 (1990).
[28] E. A. Guggenheim, J. Chem. Phys. **13**, 253 (1945).
[29] A. Lotfi, J. Vrabec, and J. Fischer, Mol. Phys. **76**, 1319 (1992).
[30] J. P. Hansen and L. Verlet, Phys. Rev. **184**, 151 (1994).
[31] R. J. F. Letoe de Carvalho, R. Evans, D. C. Hoyle, and J. R. Henderson, J. Phys. Condens. Matter, **6**, 9275 (1994).
[32] S. H. Sung and D. Chandler, Phys. Rev. A **9**, 1688 (1974).